World Journal of Gastroenterology

Online Submissions: http://www.wjgnet.com/esps/
wjg@wjgnet.com
doi:10.3748/wjg.v18.i40.5821

World J Gastroenterol 2012 October 28; 18(40): 5821-5825
ISSN 1007-9327 (print) ISSN 2219-2840 (online)

CASE REPORT

Different imaging findings of inflammatory myofibroblastic tumor of the liver

Xiao-Fei Liu, Bao-Ming He, Xiao-Hui Ou-Yang, Zhi-Zhong Wang, Jia-Gui Su

Xiao-Fei Liu, Bao-Ming He, Xiao-Hui Ou-Yang, Zhi-Zhong Wang, Jia-Gui Su, Department of Nuclear Medicine, The People's Liberation Army 309th Hospital, Beijing 100091, China
Author contributions: Liu XF and He BM designed the research; Ou-Yang XH, Wang ZZ and Su JG contributed analytical tools; Liu XF and He BM wrote the paper.
Correspondence to: Bao-Ming He, MD, Department of Nuclear Medicine, The People's Liberation Army 309th Hospital, Beijing 100091, China. liufly301@163.com
Telephone: +86-10-51520604 Fax: +86-10-51520931
Received: May 12, 2012 Revised: August 6, 2012
Accepted: August 14, 2012
Published online: October 28, 2012

Abstract

Inflammatory myofibroblastic tumor (IMT) in the liver is an uncommon lesion of uncertain pathogenesis. In most cases, symptomatological imaging and clinical studies suggest malignancy. We report a case of liver IMT with imaging findings from positron emission tomography/computed tomography (PET/CT), contrast-enhanced computed tomography (CECT) and contrast-enhanced ultrasonography (CEUS). This report was the first to depict a PET/CT scan of a liver IMT that revealed an inhomogeneous, intense (fluorine 18)-fluoro-2-deoxy-D-glucose uptake. The CECT and CEUS images showed a hepatic artery supplying blood to the mass and necrosis. The characteristic histopathological features and the presence of spindle cells expressing smooth muscle actin, collagen fibers and lymphocytes allowed for the diagnosis of liver IMT. Recognizing such findings will help to achieve a correct diagnosis and may prevent inappropriate treatment.

Key words: Inflammatory myofibroblastic tumor; Liver; Emission-computed tomography; X-ray-computed tomography

Peer reviewer: Ming-Lung Yu, MD, PhD, Professor, Division of Hepatology, Department of Medicine, Kaohsiung Medical University Hospital, 100 Tzyou 1st Rd, Kaohsiung 807, Taiwan, China

Liu XF, He BM, Ou-Yang XH, Wang ZZ, Su JG. Different imaging findings of inflammatory myofibroblastic tumor of the liver. *World J Gastroenterol* 2012; 18(40): 5821-5825 Available from: URL: http://www.wjgnet.com/1007-9327/full/v18/i40/5821.htm DOI: http://dx.doi.org/10.3748/wjg.v18.i40.5821

INTRODUCTION

Inflammatory myofibroblastic tumor (IMT) is rare. Although IMT was once considered a soft tissue lesion, it has also been reported in the mesentery, omentum, major salivary glands, larynx, breast and thyroid gland, and in visceral organs, such as the lung, small intestine and kidney. To date, the appearance of IMT in the liver has been minimal[1]. Because of how it appears on different types of imaging, IMT is difficult to clinically differentiate from malignant tumors. IMT may regress spontaneously; therefore, indications for surgery must be carefully assessed. Cases involving (fluorine 18)-fluoro-2-deoxy-D-glucose positron emission tomography and computed tomography (^{18}F-FDG-PET/CT) examinations of liver IMT have never been reported. Here, we report a case of liver IMT using ^{18}F-FDG-PET/CT, contrast-enhanced computed tomography (CECT) and contrast-enhanced ultrasonography (CEUS). The imaging findings showed a hepatic artery supplying blood to the mass in the presence of necrosis. An inhomogeneous, intense ^{18}F-FDG uptake was also noted. The characteristic histopathological features, along with the presence of spindle cells expressing smooth muscle actin (SMA), collagen fibers and lymphocytes, allowed for the IMT diagnosis. Recognizing such findings will improve correct diagnosis and may prevent inappropriate treatment.

CASE REPORT

A 42-year-old Chinese woman presented with high fever (39 ℃) and denied having abdominal pain, fatigue and weight loss. On physical examination, the right upper quadrant of the patient's liver was tender at palpation. After being placed on anti-infection medicine, her body temperature decreased to a maintainable range (within normal limits). However, when the treatment ceased, the original fever returned. The laboratory results revealed a white blood cell count of 10 900/mL with segmental neutrophilia (73.4%) and slightly elevated levels of C-reactive protein (CRP, 116.2 mg/L) and fibrinogen (5.191 g/L); the erythrocyte sedimentation rate (ESR) and hemoglobin level (7.4 g/dL) were normal. The liver function tests were within the normal limits, as were the tests for alpha-fetoprotein (AFP, 2.0 ng/mL), carbohydrate antigen 19-9 (CA19-9, 13.84 U/mL), CA125 (17.71 U/mL), CA50 (12.4 U/mL) and carcinoembryonic antigen (CEA, 1.91 ng/mL). The serology markers for hepatitis and infectious agents such as echinococcus were also negative.

Conventional ultrasonography (CUS, ProSound SSD Alpha 10 system designed by Aloka Co, Ltd, Tokyo, Japan) revealed that there was a 3.8 cm × 4.6 cm hypoechoic mass in the right anterior lobe of the liver that had a clearly defined border and a heterogeneous echo texture. CEUS examinations were performed after the CUS by administering a sulfur hexafluoride-filled microbubble contrast agent (SonoVue; Bracco SpA, Milan, Italy). After administering the contrast agent, the arterial phase images showed hyperenhancement of the mass. The portal phase and parenchymal phase images revealed wash-out that corresponded to that on the arterial phase images. On the edge of the mass, there was a 1.3 cm × 1.5 cm solid nodule with a strong echo and a clear border that did not show signs of either parenchymal or arterial phases. CEUS indicated that the mass had a rich blood supply and necrosis, which is typical of a malignant tumor (Figure 1).

The patient had a whole-body ^{18}F-FDG PET/CT (Discovery VCT, GE, American) scan that returned normal results for all of the organs except the liver. The imaging showed an inhomogeneous, intense uptake of ^{18}F-FDG with SUVmax 9.1 (SUV standardized uptake value) in the anterior segment of the right lobe of the liver (Figure 2). The inhomogeneous uptake of the mass was more intense at its periphery. The mass size was approximately 4.9 cm × 4.6 cm × 5.0 cm. An abdominal CECT confirmed tumor localization in the anterior segment of the right lobe of the liver and showed that enhancement of the mass was broad and well defined at its periphery in the arterial phase. Portal venous phase images depicted a further enhancing mass, while the delayed-phase images revealed a quick wash-out that corresponded to the observations from the arterial-phase images. They were not as prevalent as those reported during the portal venous phase. There was evidence of necrosis in front of the mass and a liver lobe artery at the periphery of the mass. A 1.6 cm × 1.5 cm low-density nodule that had not been illuminated during either of the phases was present on the front edge of the mass (Figure 3).

Laparoscopy indicated that the mass was protruding from the liver surface and was slightly adhered to the surrounding tissue. The mass color was yellowish; however, it did not cause congestion or edema, and the common bile duct was not enlarged. The gall bladder, stomach, spleen, colon, small intestine and other organs were normal. A right lobectomy of the liver was performed by laparoscopy, and the mass was completely resected because the minimal contact it had with the large vessels minimized the risk. A portion of the free necrotic liver tissue was removed. Doctors dissected the specimen, which was approximately 6 cm in diameter.

Upon closer pathological examination, the mass measured 4.5 cm × 4.3 cm × 3.5 cm and weighed 1.6 kg; it was easily removed from the surrounding parenchyma. A microscopic examination revealed that the mass was composed of collagen fibers, chronic inflammatory cells lying on loose T-lymphocytes and ganglion-like cells. The chronic inflammatory infiltrate was characterized by the predominant proliferation of plasma cells in addition to lymphocytes and collagen fibers. An immunohistochemical analysis revealed that the spindle cells were positive for SMA and that the ganglion cell-like cells were positive for neuron-specific enolase and S-100. Staining for P53, desmin and epithelial membrane antigen was negative. The histological patterns were fibrous histiocytoma-like and desmoid-type (Figure 4).

DISCUSSION

IMT is a lesion with intermediate biological behavior that may recur with local or surrounding infiltration or, in rare cases, metastasis. IMT has been observed in almost all solid organs; however, its incidence in the liver has been low[1]. The case presented here involved a 42-year-old woman with a mass located on the right lobe of the liver; according to the pathological and immunohistochemical findings, the mass was diagnosed as IMT. One and a half years after surgery, no recurrence or metastasis have been identified.

This case contradicted the frequent male predilection of the lesion (male/female: 1.5/1), demonstrating that liver IMT was not limited to younger age groups and males[1]. Clinical findings indicate that symptoms in most cases include fever, abdominal pain, weight loss, weakness, and anorexia. Laboratory investigations usually suggest an inflammatory process: leukocytosis, neutrophilia, elevated ESR and CRP, anemia, thrombocytosis, polyclonal hypergammaglobulinemia, and slightly elevated levels of liver enzymes. Tumor markers, such as serum AFP and CEA, are always normal. Although these markers are valuable in the discrimination of liver IMT from malignant tumors, they cannot completely rule out some malignancies in which AFP levels may also be normal, such as fibrolamellar hepatocellular carcinoma. In this

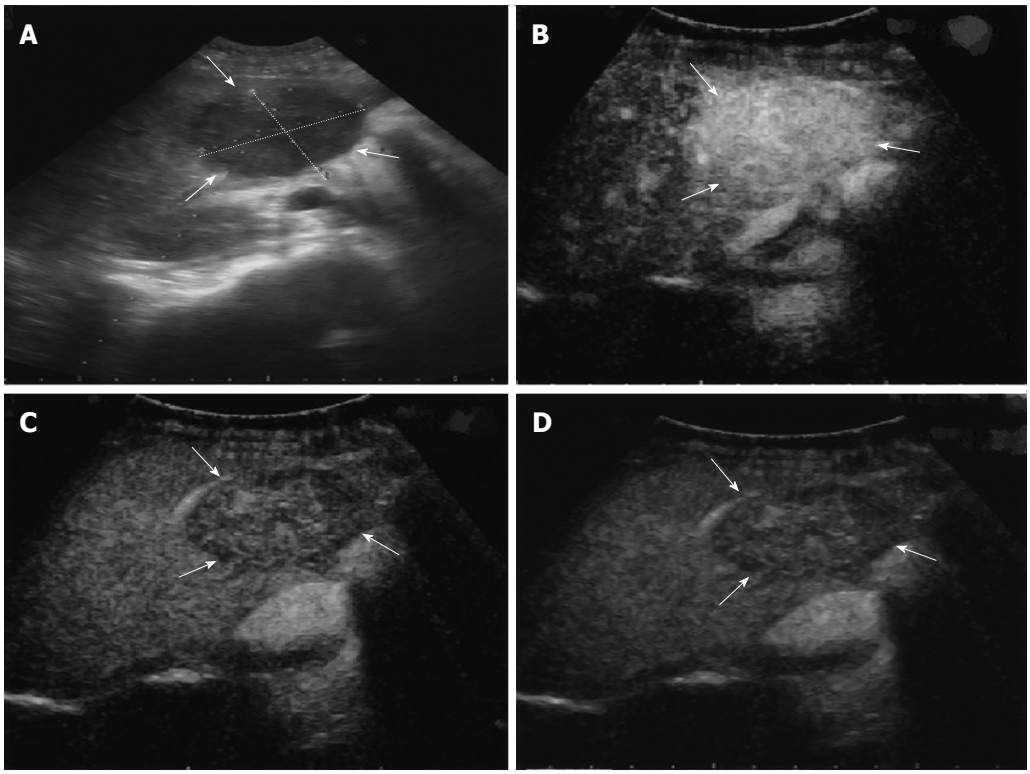

Figure 1 Ultrasonography images of the liver inflammatory myofibroblastic tumor. A: Conventional ultrasonography showing a 3.8 cm × 4.6 cm hypoechoic mass in the right anterior lobe of the liver, with a clearly defined border (white arrows); B: Arterial-phase images showing a hyperenhanced mass on the liver (white arrows); C: Portal venous-phase images showing slight enhancement and wash-out of the mass, which corresponded to that seen on arterial-phase images (white arrows); D: Parenchymal-phase images showing further wash-out of the mass, which corresponded to that on arterial-phase images (white arrows).

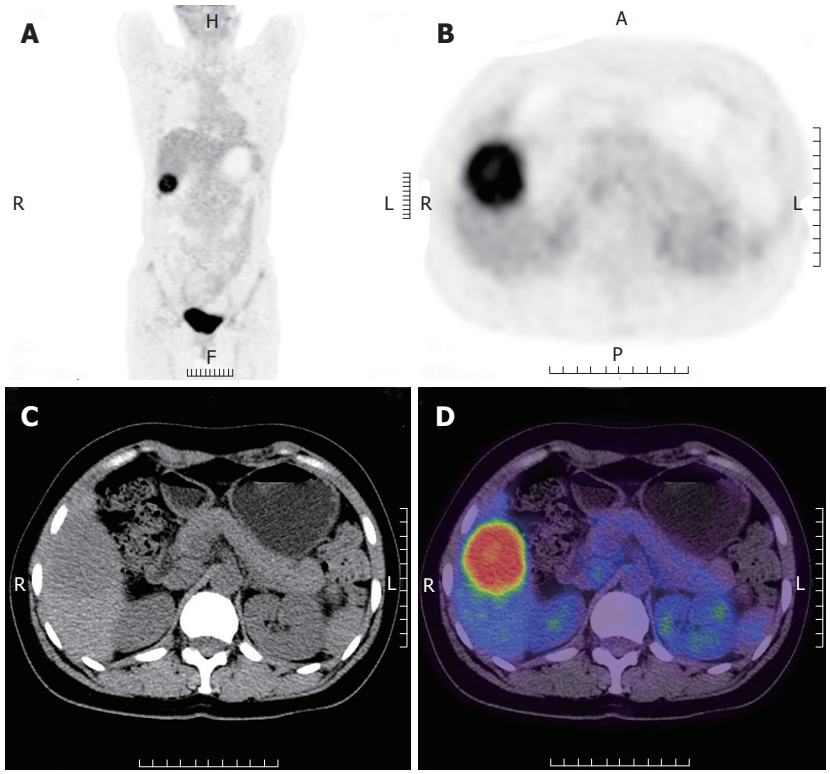

Figure 2 (Fluorine 18) fluoro-2-deoxy-D-glucose positron emission tomography and computed tomography images of the liver inflammatory myofibroblastic tumor. A: Coronal positron emission tomography (PET) demonstrating an intense (fluorine 18) fluoro-2-deoxy-D-glucose (^{18}F-FDG) uptake with SUV standardized uptake value in the anterior segment of right lobe of the liver; B: Axial PET demonstrating an inhomogeneous intense ^{18}F-FDG uptake; C: Axial computed tomography (CT) demonstrating a round mass with low density; D: Axial PET/CT demonstrating an inhomogeneous intense ^{18}F-FDG uptake in the anterior segment of right lobe. R: Right; L: Left; A: Anterior, P: Posterior; H: Head; F: Foot.

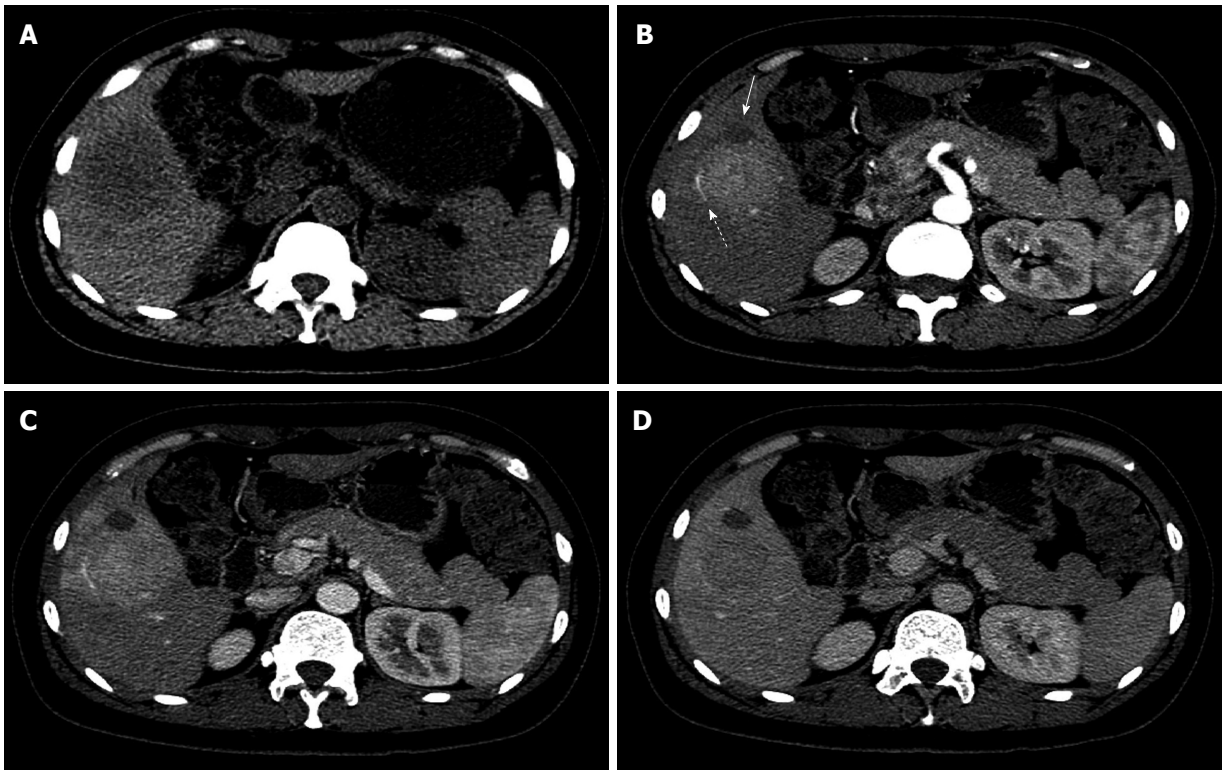

Figure 3 Axial contrast enhanced computed tomography images of the liver inflammatory myofibroblastic tumor. A: Axial arterial phase images showing a hyperenhanced mass well defined at the periphery of the mass; B: Arterial phase images showing a liver lobe artery (dash arrow) around the mass and the front edge of the mass lay a low density nodule (solid arrow) not enhancing in three phase images; C: Axial portal venous phase images showing a further enhanced corresponding to the arterial phase images; D: Axial delayed images showing obviously wash-out corresponding to the arterial phase images.

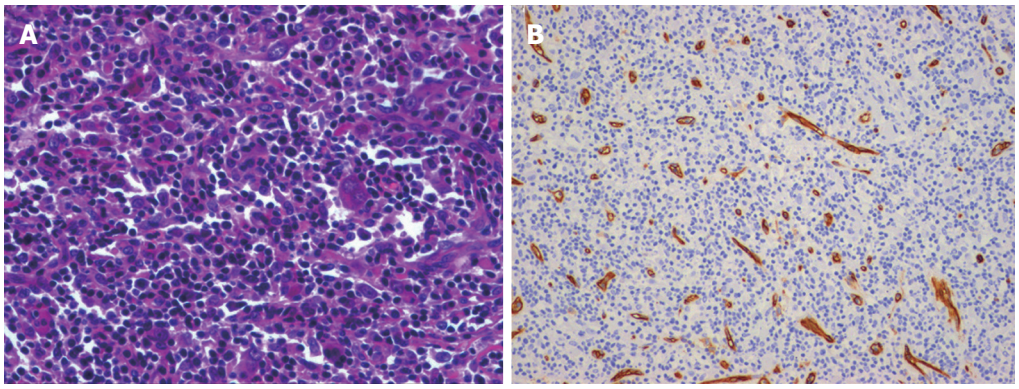

Figure 4 Histopathology findings of the liver inflammatory myofibroblastic tumor. A: Lesion was composed of chronic inflammatory cells and spindle cells (hematoxylin and eosin stain, × 200); B: Spindle cells were positive in smooth muscle actin tumor (immunostaining, × 100).

case, the clinical symptoms were nonspecific. The patient denied having abdominal pain, fatigue and weight loss. As described in the laboratory setting, the aminotransferases were all normal.

Furthermore, radiological aspects of IMT are usually similar to those of a malignant neoplasm[2]. Mali *et al*[3] reported a homogeneous mass without calcification or contrast enhancement. Megumi *et al*[4] reported that CECT revealed a soft, deeply stained image on the margin of the mass in the early phase. In the late phase, enhancement of the center of the mass was poor, and there was a soft, deeply stained image around the center. In this case, the CECT showed a hyperenhanced image in the arterial phase and a further developing mass in the portal venous phase; the contrast was obviously washed out in the delayed phase. On the front edge of the mass lay a low-density nodule, indicating the necrotic liver tissue that was removed by the surgeon, which has never been reported. However, the CECT image results of our case conflicted with the above case reports. These findings support the notion that the IMT CT image findings were nonspecific and could mimic many diseases.

Nam *et al*[5,6] observed two different appearances of the hepatic IMT. The enhancement was broad and ill-

defined at the periphery of the mass. In our case, the enhancement was broad and well defined at the periphery of the mass. In agreement with the histopathologic findings, the hypo-enhanced areas identified in the CECT correlated with the concentrated fibrous tissue, and the hyper-enhanced area corresponded predominantly with the cellular infiltration that contained foamy histiocytes, plasma cells, and lymphocytes. These image and pathological results corresponded to the findings in this study. To our knowledge, there has been no report on liver IMT with PET/CT. Wan *et al*[7] reported that inflammatory tissue has high metabolic activity. In addition, this case demonstrated an inhomogeneous, intense ^{18}F-FDG uptake with SUVmax 9.1. The inhomogeneous ^{18}F-FDG uptake of the mass corresponded to the different mass components (collagen fibers, chronic inflammatory cells, T-lymphocytes, ganglion-like cells).

IMT may be more difficult to clinically differentiate from malignant tumors, and different types of image findings and an excision biopsy may frequently be needed to make the diagnosis. The postoperative prognosis of liver IMT is favorable[4]. Some reports have shown that percutaneous needle biopsies are efficient for making the diagnosis[8]. When malignant tumors are suspected, a needle biopsy is not necessarily recommended because there is a risk of tumor cell dissemination. Because it may show spontaneous regression, indications for surgery must be carefully assessed. It is important that similar clinical cases perform ^{18}F-FDG PET/CT, CECT or MRI.

The pathogenesis of IMT is uncertain. Some authors have suggested an infectious origin; however, few cases have provided positive cultures or microorganisms isolated from tissue sections[2]. It was suggested that the chronic xanthogranulomatous pattern was a response to a previous infectious process. IMT can occur after surgery, trauma, radiotherapy or steroid use; it can also occur in connection with ventriculo-peritoneal shunts or infectious agents, such as *Mycobacterium avium intracellulare*, *Corynebacterium equi*, *Campylobacter jejuni*, *Bacillus sphaericus*, *Coxiella burnetii*, *Epstein-Barr* virus, *Escherichia coli*, *human herpes* virus 8 and *Actinomycosis*[3,9,10]. Some IMT cases are related to infectious or reparative processes, and the association of IMT with some infectious agents has been related to its pathogenesis, although it is rarely observed. According to some authors[6], IMT could develop secondary portal venous infection, and the inflammatory mass might enlarge together with the obliterative phlebitis, which may explain the tumoral development in the patient. As previously described in the literature, this tumor was found in the right lobe of the liver and was characterized by a well-circumscribed firm lesion with myxoid areas and a yellow or whitish color. Fleshy or myxoid surfaces suffering from lacerations rarely exhibit hemorrhage, necrosis or calcification[1]; however, this case showed necrotic liver tissue on the CECT and the CEUS, and this necrotic tissue was removed by our surgeon. The differential diagnosis depends upon the histological patterns observed; although we observed a hypocellular fibrous pattern with some inflammatory cells, the SMA immunoreactivity in the spindle cells was important in the diagnosis. CD34, CD23 and CD117 were non-immunoreactive in the spindle cells, which excluded the diagnosis of a fibrous solitary tumor. Although ganglion-like cells were positive in this case, there was no malignant tendency.

In this case, there was notable evidence of necrosis in front of the mass and a lobe artery at the periphery of the mass, which sometimes relates to malignant tumors. Although clinical, histopathological or molecular features do not predict biological behavior[10], recurrences are associated with the abdominal site, large size of the tumor and older age. Because the tumor may regress spontaneously, indications for surgery must be carefully assessed. Although ^{18}F-FDG PET/CT examinations can successfully differentiate IMT from other types of malignant tumors, the appropriate method of diagnosing liver IMT is still *via* histopathologic examination.

REFERENCES

1 **Sürer E**, Bozova S, Gökhan GA, Gürkan A, Elpek GO. Inflammatory myofibroblastic tumor of the liver: a case report. *Turk J Gastroenterol* 2009; **20**: 129-134

2 **Yamrubboon W**, Phongkitkarun S, Jaovisidha S, Sirikulchayanonta V, Tapaneeyakorn J, Siripornpitak S. Inflammatory myofibroblastic tumor ofabdomen: computerized tomographic (CT) and pathological findings. *J Med Assoc Thai* 2008; **91**: 1487-1493

3 **Mali VP**, Tan HC, Loh D, Prabhakaran K. Inflammatory tumour of the retroperitoneum--a case report. *Ann Acad Med Singapore* 2005; **34**: 632-635

4 **Motojuku M**, Oida Y, Morikawa G, Hoshikawa T, Nakamura T, Tajima T, Mukai M, Otsuka H, Akieda K, Hirabayashi K, Makuuchi H, Inokuchi S. Inflammatory pseudotumor of the liver: case report and review of literature. *Tokai J Exp Clin Med* 2008; **33**: 70-74

5 **Nam KJ**, Kang HK, Lim JH. Inflammatory pseudotumor of the liver: CT and sonographic findings. *AJR Am J Roentgenol* 1996; **167**: 485-487

6 **Yoon KH**, Ha HK, Lee JS, Suh JH, Kim MH, Kim PN, Lee MG, Yun KJ, Choi SC, Nah YH, Kim CG, Won JJ, Auh YH. Inflammatory pseudotumor of the liver in patients with recurrent pyogenic cholangitis: CT-histopathologic correlation. *Radiology* 1999; **211**: 373-379

7 **Wan DQ**, Xu AD, Manner CE. False positive for malignancy of a lung nodule on FDG PET/CT scans--a lesion with high FDG uptake but stable in size. *Clin Imaging* 2010; **34**: 393-395

8 **Takamori R**, Wong LL, Dang C, Wong L. Needle-tract implantation from hepatocellular cancer: is needle biopsy of the liver always necessary? *Liver Transpl* 2000; **6**: 67-72

9 **Radhi J**, Hadjis N, Anderson L, Burbridge B, Ali K. Retroperitoneal actinomycosis masquerading as inflammatory pseudotumor. *J Pediatr Surg* 1997; **32:** 618-620

10 **Arber DA**, Kamel OW, van de Rijn M, Davis RE, Medeiros LJ, Jaffe ES, Weiss LM. Frequent presence of the Epstein-Barr virus in inflammatory pseudotumor. *Hum Pathol* 1995; **26**: 1093-1098

S- Editor Gou SX **L- Editor** A **E- Editor** Xiong L